CONSTRAINED MAXIMUM DIRECTIVITY BEAMFORMERS BASED ON UNIFORM LINEAR ACOUSTIC VECTOR SENSOR ARRAYS

Xueqin Luo[1], *Jilu Jin*[1], *Gongping Huang*[2], *Jingdong Chen*[1], *Jacob Benesty*[3], *Israel Cohen*[2], *Wen Zhang*[1]

[1]CIAIC and Shaanxi Provincial Key Laboratory of Artificial Intelligence, Northwestern Polytechnical University, Xi'an, Shaanxi 710072, China
[2]Faculty of Electrical and Computer Engineering, Technion–Israel Institute of Technology, Technion City, Haifa 3200003, Israel
[3]INRS-EMT, University of Quebec, Montreal, QC H5A 1K6, Canada

ABSTRACT

This paper studies the problem of beamforming with linear arrays consisting of acoustic vector sensors for speech signal acquisition. It presents a beamforming method, which maximizes the directivity factor (DF) in two steps. In the first step, the same weighting filter is applied to each vector sensor so that all the vector sensors in the linear array have the same spatial response, which is steered to a look direction in the three-dimensional space. Then, a beamformer is designed in the second step to maximize the DF while constraining the gain of the beampattern to be maximum at the look direction. The resulting maximum DF (MDF) beamformer has many advantages over the traditional superdirective beamformer with linear arrays of omnidirectional sensors including, but not limited to: 1) it has better steering flexibility and its mainlobe can be steered to any direction in the three-dimensional space, while the traditional superdirective beamformer generally has its mainlobe placed in the endfire directions; 2) it is able to achieve a high DF with the same level of white noise gain. Simulations validate the theoretical study and demonstrate the properties of the presented method.

Index Terms— Acoustic vector sensor, beamforming, superdirective, directivity factor, white noise gain.

1. INTRODUCTION

Microphone arrays have been widely used in various acoustic applications for sound source localization and audio/speech signal enhancement [1–4]. One important factor that deserves a careful attention in the design of microphone array systems is the array topology (also called geometry), the selection of which depends not only on the functionality and performance requirements, but also on the size and shape of the devices in which the array will be embedded. Among the many different types of topologies that have been investigated in the literature, e.g., linear [2–4], circular [5–9], concentric circular [8, 10, 11], planar [12–15], cubic, and spherical [16–18] ones, to name but a few, the linear topology is the most appropriate for thin devices such as smart televisions/panels/pads, etc. Consequently, over the last few decades a great deal of effort has been devoted to the design of linear arrays and the development of the associated beamforming methods, which include the superdirective [19–24], differential [11,25–28], frequency-invariant [8,29–32], and adaptive [33–37] beamformers.

However, the existing linear microphone array systems, which consist of omnidirectional sensors, generally suffer from two great limitations: 1) their performance in terms of noise and interference suppression varies significantly with the steering angle; and 2) the beampattern can only be steered within the sensors' plane and cannot be controlled in the plane orthogonal to the sensors' plane regardless what beamforming method is used. There are two major ways to remedy these drawbacks. The first one is to change the topology from linear to two-dimensional or three-dimensional ones, and the second way is to use acoustic vector sensors (AVSs).

In this work we adopt the second method and study the beamforming problem with uniform linear AVS arrays (ULAVSAs). We present a beamforming method, which maximizes the directivity factor (DF) in two steps, which was inspired by the ideas in [38–41]. In the first step, the same weighting filter is applied to each AVS so that all the AVSs in the linear array have the same spatial response, which is steered to a look direction in the three dimensional space. In the second step, a beamformer is designed to maximize the DF while constraining the derivative of the beampattern to be zero at the look direction [42]. This method can be viewed as an extension of the traditional superdirective beamformer from linear arrays with omnidirectional sensors to those with AVSs. In comparison with the traditional superdirective beamformer, the presented maximum DF (MDF) beamformer offers a number of advantages. First, it has better steering flexibility thanks to the inherent three-dimensional directivity of each AVS and its mainlobe can be steered to any direction in the three dimensional space while the traditional superdirective beamformer generally has its mainlobe placed in the endfire directions; 2) it is able to achieve a high DF with the same level of white noise gain (WNG).

2. SIGNAL MODEL, PROBLEM FORMULATION, AND PERFORMANCE METRICS

Let us consider a far-field plane wave that propagates in an anechoic environment at the speed of sound, i.e., $c = 340$ m/s, and impinges on an AVS from the elevation angle θ and azimuth angle ϕ. The AVS receives four measurements, i.e., one monopole measurement as well as three dipole measurements in x, y, z-axis, respectively. After applying a weight vector $\mathbf{w}$, the directivity pattern of an AVS can be ideally written as [39]

$$\mathcal{A}(\theta, \phi) = \mathbf{w}^H \boldsymbol{\beta}(\theta, \phi), \tag{1}$$

where the superscript ^{H} is the complex-conjugate operator and

$$\boldsymbol{\beta}(\theta, \phi) = \left[\begin{array}{cccc} 1 & \sin\theta\cos\phi & \sin\theta\sin\phi & \cos\theta \end{array} \right]^T, \tag{2}$$

with the superscript ^{T} being the transpose operator.

In our study, we consider a ULAVSA consisting of M identical AVSs. Without loss of generality, we assume that all the AVSs are placed on the z-axis and the interelement spacing between two successive AVSs is δ. We also assume that all the AVSs are weighted with the same vector $\mathbf{w}$. Then, the phase vector of the ULAVSA can be written as

$$\underline{\mathbf{d}}(\omega, \theta, \phi) = \mathcal{A}(\theta, \phi)\, \mathbf{d}(\omega, \theta), \tag{3}$$

This work was supported in part by the National Key Research and Development Program of China under Grant No. 2018AAA0102200 and in part by the Key Program of National Science Foundation of China (NSFC) under Grant No. 61831019.

where

$$\mathbf{d}(\omega,\theta)=\left[\begin{array}{cccc}1 & e^{-\jmath\varpi\cos\theta} & \cdots & e^{-\jmath(M-1)\varpi\cos\theta}\end{array}\right]^T, \quad (4)$$

ω is the angular frequency, $\jmath$ is the imaginary unit, and $\varpi=\omega\delta/c$.

The objective of beamforming is to further recover the source signal of interest that is corrupted by spatial acoustic noise. For that, the output of each AVS after being weighted with $\mathbf{w}$, is multiplied by a complex weight, $H_m^*(\omega)$ (for $m=1,2,\ldots,M$), where the superscript * is the complex-conjugate operator. The weighted outputs are then summed together to form the beamformer's output. Stacking all the weights together in a vector of length M, we get

$$\mathbf{h}(\omega)=\left[\begin{array}{cccc}H_1(\omega) & H_2(\omega) & \cdots & H_M(\omega)\end{array}\right]^T. \quad (5)$$

Then, the problem of beamforming is to find the optimal filter so that the beamformer's output is a good estimate of the source signal of interest.

The beampattern, which describes the sensitivity of a beamformer to a plane wave impinging on the array from the direction (θ,ϕ), is typically used to evaluate the performance of a beamformer. For the above beamforming process, it is defined as

$$\begin{aligned}\mathcal{B}[\mathbf{h}(\omega)|\mathbf{w},\theta,\phi]&=\mathbf{h}^H(\omega)\underline{\mathbf{d}}(\omega,\theta,\phi)\\&=\mathcal{A}(\theta,\phi)\mathbf{h}^H(\omega)\mathbf{d}(\omega,\theta).\end{aligned} \quad (6)$$

To preserve the desired signal, the distortionless constraint is applied, i.e.,

$$\mathbf{h}^H(\omega)\underline{\mathbf{d}}(\omega,\theta_{\mathrm{s}},\phi_{\mathrm{s}})=1. \quad (7)$$

In our study, we apply a frequency-independent real-valued weight vector to the AVS measurements as [27, 39, 43]

$$\mathbf{w}=\left[\begin{array}{cccc}a_0 & a_1\sin\theta_{\mathrm{s}}\cos\phi_{\mathrm{s}} & a_1\sin\theta_{\mathrm{s}}\sin\phi_{\mathrm{s}} & a_1\cos\theta_{\mathrm{s}}\end{array}\right]^T, \quad (8)$$

where $a_1=1-a_0$ and a_0 is a real coefficient, which can be adjusted to obtain different kinds of first-order directivity patterns:

$$\begin{aligned}\mathcal{A}(\theta,\phi)&=\mathbf{w}^T\boldsymbol{\beta}(\theta,\phi)\\&=a_0+a_1\left[\cos\theta_{\mathrm{s}}\cos\theta+\sin\theta_{\mathrm{s}}\sin\theta\cos(\phi-\phi_{\mathrm{s}})\right].\end{aligned} \quad (9)$$

Figure 1 shows an example of the directivity pattern of an AVS based first-order beamformer with the look direction being steered to $(\theta_{\mathrm{s}},\phi_{\mathrm{s}})$.

It is easy to check that $\mathcal{A}(\theta_{\mathrm{s}},\phi_{\mathrm{s}})=1$, so now the distortionless constraint is equivalent to

$$\mathbf{h}^H(\omega)\mathbf{d}(\omega,\theta_{\mathrm{s}})=1. \quad (10)$$

The WNG, which evaluates the sensitivity of the beamformer to some of the array imperfections, is defined for the ULAVSA as [2, 44]

$$\mathcal{W}[\mathbf{h}(\omega)|\mathbf{w}]=\alpha\frac{\left|\mathbf{h}^H(\omega)\underline{\mathbf{d}}(\omega,\theta_{\mathrm{s}},\phi_{\mathrm{s}})\right|^2}{\mathbf{h}^H(\omega)\mathbf{h}(\omega)}, \quad (11)$$

where

$$\alpha=\frac{1}{\mathbf{w}^T\mathbf{w}}. \quad (12)$$

The DF, which quantifies how directive is the beamformer's spatial response, is given by [17, 44]

$$\mathcal{D}[\mathbf{h}(\omega)|\mathbf{w}]=\frac{\left|\mathbf{h}^H(\omega)\underline{\mathbf{d}}(\omega,\theta_{\mathrm{s}},\phi_{\mathrm{s}})\right|^2}{\mathbf{h}^H(\omega)\boldsymbol{\Gamma}_{\mathrm{d}}(\omega)\mathbf{h}(\omega)}, \quad (13)$$

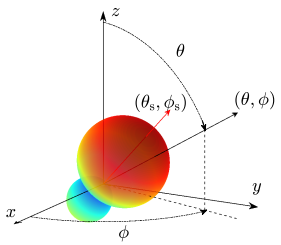

Fig. 1. Illustration of the three-dimensional directivity pattern of an AVS, which is placed at the origin of the Cartesian coordinate system and whose look direction is $(\theta_{\mathrm{s}},\phi_{\mathrm{s}})$.

where

$$\boldsymbol{\Gamma}_{\mathrm{d}}(\omega)=\frac{1}{4\pi}\int_0^{2\pi}\int_0^{\pi}\underline{\mathbf{d}}(\omega,\theta,\phi)\underline{\mathbf{d}}^H(\omega,\theta,\phi)\sin\theta d\theta d\phi.$$

It can be verified that the (i,j)th element of $\boldsymbol{\Gamma}_{\mathrm{d}}(\omega)$ is

$$\left[\boldsymbol{\Gamma}_{\mathrm{d}}(\omega)\right]_{ij}=\frac{1}{4\pi}\int_0^{2\pi}\int_0^{\pi}\left|\mathcal{A}(\theta,\phi)\right|^2e^{\gamma_{ij}\cos\theta}\sin\theta d\theta d\phi, \quad (14)$$

where $\gamma_{ij}=\jmath\varpi(j-i)$. One can deduce that

$$\left[\boldsymbol{\Gamma}_{\mathrm{d}}(\omega)\right]_{i,j}= \quad (15)$$
$$\left\{\begin{array}{ll}\frac{a_1^2}{3}+a_0^2, & i=j\\ \sum_{n=1}^{3}\xi_n\gamma_{ij}^{-n}\sinh(\gamma_{ij})+\sum_{n=1}^{2}\xi_{n+3}\gamma_{ij}^{-n}\cosh(\gamma_{ij}), & i\neq j\end{array}\right.,$$

where

$$\begin{aligned}\sinh(\gamma_{ij})&=\frac{e^{\gamma_{ij}}-e^{-\gamma_{ij}}}{2},\\ \cosh(\gamma_{ij})&=\frac{e^{\gamma_{ij}}+e^{-\gamma_{ij}}}{2},\\ \xi_1&=\frac{2a_0^2+a_1^2(\cos2\theta_{\mathrm{s}}+1)}{2},\\ \xi_2&=-\xi_4=-2a_1a_0\cos\theta_{\mathrm{s}},\\ \xi_3&=-\xi_5=\frac{a_1^2(3\cos2\theta_{\mathrm{s}}+1)}{2}.\end{aligned}$$

3. CONSTRAINED MDF BEAMFORMER

With the specified coordinate system and placement of sensors, the beampattern along the azimuth direction depends only on $\mathcal{A}(\theta,\phi)$ and does not change with respect to $\mathbf{h}(\omega)$, which can be observed from (6). Consequently, the MDF beamformer can be designed by maximizing the DF while maintaining the elevation angle of the look direction at θ_{s}. Mathematically, this maximization problem can be translated to one of finding the solution of the following equation:

$$\left.\frac{\partial\mathcal{B}[\mathbf{h}(\omega)|\mathbf{w},\theta,\phi]}{\partial\theta}\right|_{(\theta,\phi)=(\theta_{\mathrm{s}},\phi_{\mathrm{s}})}=0. \quad (16)$$

According to (6), the partial derivative of the beampattern with respect to θ on the left-hand side of (16) can be deduced as

$$\begin{aligned}\frac{\partial\mathcal{B}[\mathbf{h}(\omega)|\mathbf{w},\theta,\phi]}{\partial\theta}&=\mathbf{h}^H(\omega)\frac{\partial\underline{\mathbf{d}}(\omega,\theta,\phi)}{\partial\theta}\\&=\mathbf{h}^H(\omega)\boldsymbol{\Sigma}_M(\theta,\phi)\mathbf{d}(\omega,\theta),\end{aligned} \quad (17)$$

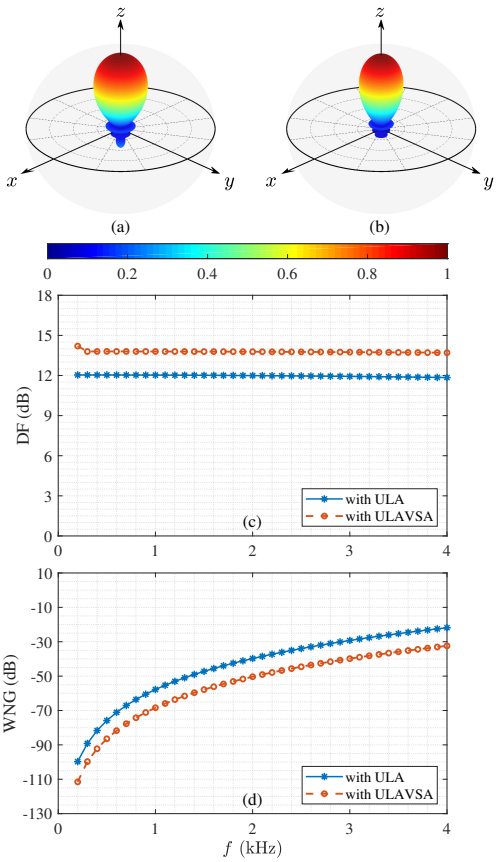

Fig. 2. Beampatterns (at $f = 1$ kHz), DF, and WNG of the constrained MDF beamformer: (a) beampattern with ULA, (b) beampattern with ULAVSA, (c) DF, and (d) WNG. Conditions: $M = 4$, $\delta = 1$ cm, and $(\theta_{\mathrm{s}}, \phi_{\mathrm{s}}) = (0^\circ, 0^\circ)$.

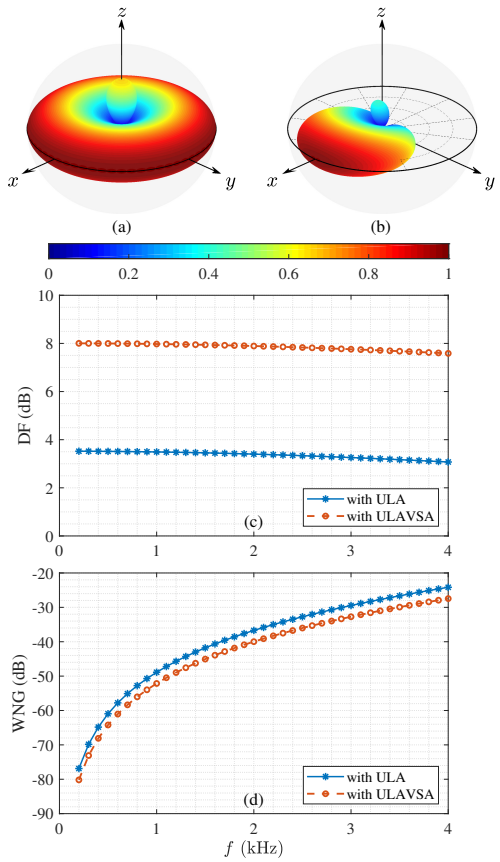

Fig. 3. Beampatterns (at $f = 1$ kHz), DF, and WNG of the constrained MDF beamformer designed with the conventional ULA and the studied ULAVSA: (a) beampattern with ULA, (b) beampattern with ULAVSA, (c) DF, and (d) WNG. Conditions: $M = 4$, $\delta = 1$ cm, and $(\theta_{\mathrm{s}}, \phi_{\mathrm{s}}) = (90^\circ, 0^\circ)$.

where $\mathbf{\Sigma}_M(\theta, \phi)$ is a diagonal matrix whose (m, m)th element is

$$[\mathbf{\Sigma}_M(\theta, \phi)]_{mm} = \jmath(m-1)\varpi \sin\theta \mathcal{A}(\theta, \phi) + \frac{\partial \mathcal{A}(\theta, \phi)}{\partial \theta}. \quad (18)$$

If $(\theta, \phi) = (\theta_{\mathrm{s}}, \phi_{\mathrm{s}})$, (18) can be simplified to

$$[\mathbf{\Sigma}_M(\theta_{\mathrm{s}})]_{mm} = \jmath(m-1)\varpi \sin\theta_{\mathrm{s}}. \quad (19)$$

It follows that (16) can be rewritten as

$$\mathbf{h}^H(\omega)\, \mathbf{\Sigma}_M(\theta_{\mathrm{s}})\, \mathbf{d}(\omega, \theta_{\mathrm{s}}) = 0. \quad (20)$$

3.1. Special Case for Endfire Design

We first consider a special case that the desired look direction is in the endfire direction, i.e., $\theta_{\mathrm{s}} = 0^\circ$. In this scenario, $[\mathbf{\Sigma}_M(\theta_{\mathrm{s}})]_{mm} = 0$ for $1 \leq m \leq M$. So, we can find the constrained MDF beamformer by maximizing the DF in (13) under the distortionless constraint in (10). This is equivalent to solving the following optimization problem:

$$\min_{\mathbf{h}(\omega)} \mathbf{h}^H(\omega)\, \mathbf{\Gamma}_{\mathrm{d}}(\omega)\, \mathbf{h}(\omega) \quad \text{s. t.} \quad \mathbf{h}^H(\omega)\, \mathbf{d}(\omega, \theta_{\mathrm{s}}) = 1. \quad (21)$$

The solution of (21) is

$$\mathbf{h}(\omega) = \frac{\mathbf{\Gamma}_{\mathrm{d}}^{-1}(\omega)\, \mathbf{d}(\omega, \theta_{\mathrm{s}})}{\mathbf{d}^H(\omega, \theta_{\mathrm{s}})\, \mathbf{\Gamma}_{\mathrm{d}}^{-1}(\omega)\, \mathbf{d}(\omega, \theta_{\mathrm{s}})}, \quad (22)$$

which is identical to the so-called superdirective beamformer [19].

3.2. General Design

Consider the more general case where $\theta_{\mathrm{s}} \in [0, 180^\circ]$. The constraint in (20) is needed to ensure that the maximum response appears at the desired look direction $(\theta_{\mathrm{s}}, \phi_{\mathrm{s}})$. As a result, the optimization problem can be expressed as

$$\min_{\mathbf{h}(\omega)} \mathbf{h}^H(\omega)\, \mathbf{\Gamma}_{\mathrm{d}}(\omega)\, \mathbf{h}(\omega) \quad \text{s. t.} \quad \mathbf{C}^H(\omega, \theta_{\mathrm{s}})\, \mathbf{h}(\omega) = \mathbf{i}_1, \quad (23)$$

where

$$\mathbf{C}(\omega, \theta_{\mathrm{s}}) = [\ \mathbf{d}(\omega, \theta_{\mathrm{s}}) \quad \mathbf{\Sigma}_M(\theta_{\mathrm{s}})\, \mathbf{d}(\omega, \theta_{\mathrm{s}})\ ] \quad (24)$$

is a matrix of size $M \times 2$ and $\mathbf{i}_1 = [\ 1 \quad 0\ ]^T$. The solution to (23) is given by

$$\mathbf{h}(\omega) = \mathbf{\Gamma}_{\mathrm{d}}^{-1}(\omega)\, \mathbf{C}(\omega, \theta_{\mathrm{s}}) \left[\mathbf{C}^H(\omega, \theta_{\mathrm{s}})\, \mathbf{\Gamma}_{\mathrm{d}}^{-1}(\omega)\, \mathbf{C}(\omega, \theta_{\mathrm{s}})\right]^{-1} \mathbf{i}_1. \quad (25)$$

To improve the robustness, the matrix $\mathbf{\Gamma}_{\mathrm{d}}(\omega)$ in (22) and (25) can be regularized as $\mathbf{\Gamma}_{\mathrm{d}}(\omega) + \epsilon \mathbf{I}_M$ where $\epsilon \geq 0$ is a regularization parameter to control the amount of diagonal loading.

4. SIMULATIONS

In this section, we study the performance of the proposed MDF beamformer. We consider a ULAVSA consisting of $M = 4$ AVSs,

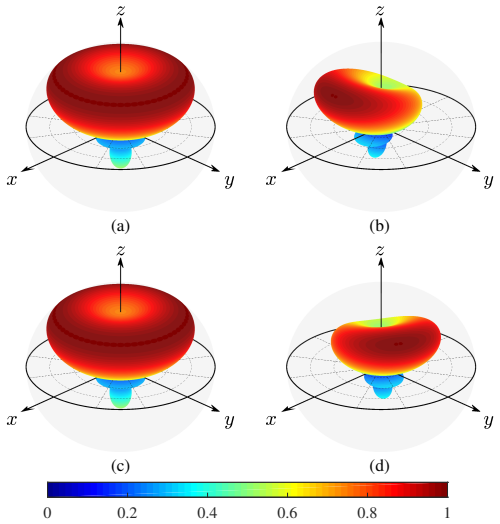

Fig. 4. Beampatterns (at $f = 1$ kHz) of the constrained MDF beamformer for different look directions: (a) with ULA, $(\theta_s, \phi_s) = (45^\circ, 0^\circ)$, (b) with ULAVSA, $(\theta_s, \phi_s) = (45^\circ, 0^\circ)$, (c) with ULA, $(\theta_s, \phi_s) = (45^\circ, 60^\circ)$, and (d) with ULAVSA, $(\theta_s, \phi_s) = (45^\circ, 60^\circ)$. Conditions: $M = 4$ and $\delta = 1$ cm.

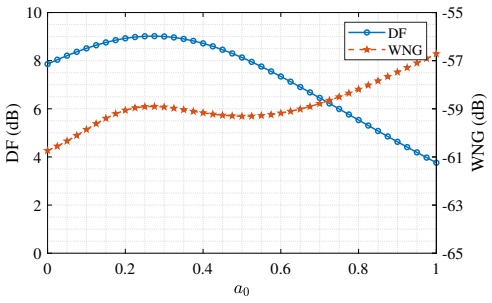

Fig. 5. DF and WNG of the constrained MDF beamformer designed with ULAVSA for different values of a_0. Conditions: $M = 4$, $\delta = 1$ cm, $(\theta_s, \phi_s) = (45^\circ, 0^\circ)$, and $f = 1$ kHz.

with an interelement spacing of $\delta = 1$ cm. For comparison, we also consider a conventional uniform linear array (ULA), with 4 omnidirectional sensors, under the same configuration. Both the ULA and ULAVSA locate at the z-axis. The constrained MDF beamformer based on ULA correspond to the case that $a_0 = 1$.

In the first simulation, the desired look direction is set as $(\theta_s, \phi_s) = (0^\circ, 0^\circ)$. A forward weight vector with $a_0 = a_1 = 1/2$ is applied to each AVS in the ULAVSA. We compare the proposed constrained MDF beamformer based on the ULAVSA with the MDF beamformer based on the conventional ULA . Figure 2 plots the beampatterns at $f = 1$ kHz, and the DF and WNG of the constrained MDF beamformers as a function of frequency. It is seen that the constrained MDF beamformer based on the ULAVSA achieves higher DFs (but note that the WNG has decreased).

In the second simulation, we set $(\theta_s, \phi_s) = (90^\circ, 0^\circ)$. The results are plotted in Fig. 3. As seen, the constrained MDF beamformer with the conventional ULA has a ring shape of main lobe at $\theta = 90^\circ$. This is understandable as the beampattern of a ULA with omnidirectional microphones is always symmetric with respect to the z-axis. In contrast, the constrained MDF beamformer with the ULAVSA generates a unique main lobe at $(90^\circ, 0^\circ)$ and achieves a much higher value of DF (but again, the WNG is lower).

To show the steering capability of the constrained MDF beamformer, Fig. 4 plots the beampatterns at $f = 1$ kHz for $(\theta_s, \phi_s) \in [(45^\circ, 0^\circ), (45^\circ, 60^\circ)]$. It is shown that the constrained MDF beamformer can achieve successful beam steering. Moreover, with the ULAVSA, the beamformer achieves higher directivities than those obtained with the ULA, and the resulting beampatterns are identical up to rotation with the same θ_s for different ϕ_s.

We can also set different values of the real coefficient a_0 in $\mathbf{w}$ to design different kinds of first-order directivity patterns. Figure 5 plots the DFs and WNGs of the constrained MDF beamformer with the ULAVSA for different values of a_0. It can be observed that the DF and WNG vary with the value of a_0; so one can optimize the performance in practical applications by tuning the parameter a_0.

5. CONCLUSIONS

This paper studied the problem of designing MDF beamformers with ULAVSAs. We first presented the signal model and corresponding performance metrics for ULAVSAs, where all AVSs have the same weight vector. We then discussed how to design a constrained MDF beamformer by maximizing the DF with a constraint on the derivative of the beampattern so that the mainlobe of the designed beamformer can be steered to different directions in the three-dimensional space. We have demonstrated by simulations that the proposed beamformer designed with ULAVSAs achieves better steering flexibility and higher directivity compared to the conventional ULA with the same number of sensors.

6. REFERENCES

[1] B. D. Van Veen and K. M. Buckley, "Beamforming: A versatile approach to spatial filtering," *IEEE ASSP Mag.*, vol. 5, pp. 4–24, Apr. 1988.

[2] M. Brandstein and D. Ward, *Microphone Arrays: Signal Processing Techniques and Applications*. Berlin, Germany: Springer-Verlag, 2001.

[3] J. Benesty, J. Chen, and Y. Huang, *Microphone Array Signal Processing*. Berlin, Germany: Springer-Verlag, 2008.

[4] J. Benesty, I. Cohen, and J. Chen, *Fundamentals of Signal Enhancement and Array Signal Processing*. Singapore: Wiley-IEEE Press., 2018.

[5] J. Meyer, "Beamforming for a circular microphone array mounted on spherically shaped objects," *J. Acoust. Soc. Am.*, vol. 109, pp. 185–193, Jan. 2001.

[6] H. Teutsch and W. Kellermann, "Acoustic source detection and localization based on wavefield decomposition using circular microphone arrays," *J. Acoust. Soc. Am.*, vol. 120, pp. 2724–2736, Nov. 2006.

[7] M. Kleider, B. Rafaely, B. Weiss, and E. Bachmat, "Golden-ratio sampling for scanning circular microphone arrays," *IEEE Trans. Audio, Speech, Lang. Process.*, vol. 18, pp. 2091–2098, Nov. 2010.

[8] G. Huang, J. Chen, and J. Benesty, "Insights into frequency-invariant beamforming with concentric circular microphone arrays," *IEEE/ACM Trans. Audio, Speech, Lang. Process.*, vol. 26, no. 12, pp. 2305–2318, 2018.

[9] Y. Wang, Y. Yang, Y. Ma, Z. He, and Y. Liu, "Broadband pattern synthesis for circular sensor arrays," *J. Acoust. Soc. Am.*, vol. 136, no. 2, pp. EL153–EL158, 2014.

[10] S. Chan and H. Chen, "Uniform concentric circular arrays with frequency-invariant characteristics: theory, design, adaptive beamforming and doa estimation," *IEEE Trans. Signal Process.*, vol. 55, no. 1, pp. 165–177, 2007.

[11] G. Huang, J. Benesty, and J. Chen, "Design of robust concentric circular differential microphone arrays," *J. Acoust. Soc. Am.*, vol. 141, no. 5, pp. 3236–3249, 2017.

[12] B. P. Kumar and G. Branner, "Generalized analytical technique for the synthesis of unequally spaced arrays with linear, planar, cylindrical or spherical geometry," *IEEE Trans. Antennas and Propagation*, vol. 53, pp. 621–634, 2005.

[13] P. J. Bevelacqua and C. A. Balanis, "Geometry and weight optimization for minimizing sidelobes in wideband planar arrays," *IEEE Trans. Antennas and Propagation*, vol. 57, pp. 1285–1289, 2009.

[14] M. Crocco and A. Trucco, "Design of superdirective planar arrays with sparse aperiodic layouts for processing broadband signals via 3-d beamforming," *IEEE Trans. Audio, Speech, Lang. Process.*, vol. 22, pp. 800–815, 2014.

[15] G. Huang, J. Chen, and J. Benesty, "Design of planar differential microphone arrays with fractional orders," *IEEE/ACM Trans. Audio, Speech, Lang. Process.*, vol. 28, 2020.

[16] J. Meyer and G. Elko, "A highly scalable spherical microphone array based on a orthonormal decomposition of the soundfield," in *Proc. IEEE ICASSP*, pp. II178–II1784, 2002.

[17] G. W. Elko and J. Meyer, "Microphone arrays," in *Springer Handbook of Speech Processing* (J. Benesty, M. M. Sondhi, and Y. Huang, eds.), ch. 48, pp. 1021–1041, Berlin, Germany: Springer-Verlag, 2008.

[18] B. Rafaely, *Fundamentals of Spherical Array Processing*. Berlin, Germany: Springer-Verlag, 2015.

[19] H. Cox, R. M. Zeskind, and T. Kooij, "Practical supergain," *IEEE Trans. Acoust., Speech, Signal Process.*, vol. 34, no. 3, pp. 393–398, 1986.

[20] G. W. Elko, "Superdirectional microphone arrays," in *Acoustic Signal Processing for Telecommunication* (S. L. Gay and J. Benesty, eds.), pp. 181–237, Berlin, Germany: Springer-Verlag, 2000.

[21] N. Stefanakis, "Efficient implementation of superdirective beamforming in a half-space environment," *J. Acoust. Soc. Am.*, vol. 145, no. 3, pp. 1293–1302, 2019.

[22] A. Atkins, Y. Ben-Hur, I. Cohen, and J. Benesty, "Robust superdirective beamformer with optimal regularization," in *Proc. IEEE IWAENC*, pp. 1–5, 2016.

[23] S. Doclo and M. Moonen, "Superdirective beamforming robust against microphone mismatch," *IEEE Trans. Acoust., Speech, Signal Process.*, vol. 15, no. 2, pp. 617–631, 2007.

[24] M. Crocco and A. Trucco, "Stochastic and analytic optimization of sparse aperiodic arrays and broadband beamformers with robust superdirective patterns," *IEEE Trans. Audio, Speech, Lang. Process.*, vol. 20, pp. 2433–2447, 2012.

[25] G. W. Elko, "Differential microphone arrays," in *Audio Signal Processing for Next-Generation Multimedia Communication Systems* (Y. Huang and J. Benesty, eds.), pp. 11–65, Berlin, Germany: Springer-Verlag, 2004.

[26] J. Benesty and J. Chen, *Study and Design of Differential Microphone Arrays*. Berlin, Germany: Springer-Verlag, 2012.

[27] J. Chen, J. Benesty, and C. Pan, "On the design and implementation of linear differential microphone arrays," *J. Acoust. Soc. Am.*, vol. 136, pp. 3097–3113, Dec. 2014.

[28] G. Huang, J. Benesty, I. Cohen, and J. Chen, "A simple theory and new method of differential beamforming with uniform linear microphone arrays," *IEEE/ACM Trans. Audio, Speech, Lang. Process.*, vol. 28, no. 1, pp. 1079–1093, 2020.

[29] S. Yan, Y. Ma, and C. Hou, "Optimal array pattern synthesis for broadband arrays," *J. Acoust. Soc. Am.*, vol. 122, no. 5, pp. 2686–2696, 2007.

[30] S. Yan, "Optimal design of modal beamformers for circular arrays," *J. Acoust. Soc. Am.*, vol. 138, no. 4, pp. 2140–2151, 2015.

[31] G. Huang, J. Benesty, and J. Chen, "On the design of frequency-invariant beampatterns with uniform circular microphone arrays," *IEEE/ACM Trans. Audio, Speech, Lang. Process.*, vol. 25, no. 5, pp. 1140–1153, 2017.

[32] H. Sun, W. Kellermann, E. Mabande, and K. Kowalczyk, "Localization of distinct reflections in rooms using spherical microphone array eigenbeam processing," *J. Acoust. Soc. Am.*, vol. 131, pp. 2828–2840, April 2012.

[33] J. Li and P. Stoica, *Robust adaptive beamforming*. Wiley Online Library, 2006.

[34] S. Markovich, S. Gannot, and I. Cohen, "Multichannel eigenspace beamforming in a reverberant noisy environment with multiple interfering speech signals," *IEEE Trans. Audio, Speech, Lang. Process.*, vol. 17, no. 6, pp. 1071–1086, 2009.

[35] E. A. P. Habets, J. Benesty, I. Cohen, S. Gannot, and J. Dmochowski, "New insights into the MVDR beamformer in room acoustics," *IEEE Trans. Audio, Speech, Lang. Process.*, vol. 18, no. 1, p. 158, 2010.

[36] S.-J. Kim, A. Magnani, A. Mutapcic, S. P. Boyd, and Z. Q. Luo, "Robust beamforming via worst-case SINR maximization," *IEEE Trans. Signal Process.*, vol. 56, no. 4, pp. 1539–1547, 2008.

[37] A. I. Koutrouvelis, R. C. Hendriks, R. Heusdens, and J. Jensen, "A convex approximation of the relaxed binaural beamforming optimization problem," *IEEE/ACM Trans. Audio, Speech, Lang. Process.*, vol. 27, no. 2, pp. 321–331, 2019.

[38] B. A. Cray and A. H. Nuttall, "Directivity factors for linear arrays of velocity sensors," *J. Acoust. Soc. Am.*, vol. 110, no. 1, pp. 324–331, 2001.

[39] D. Levin, E. A. P. Habets, and S. Gannot, "Maximum likelihood estimation of direction of arrival using an acoustic vector-sensor," *J. Acoust. Soc. Am.*, vol. 131, no. 2, pp. 1240–1248, 2012.

[40] J. Cao, A. W. H. Khong, and S. Gannot, "On the performance of widely linear quaternion based MVDR beamformer for an acoustic vector sensor," in *Proc. IEEE IWAENC*, pp. 303–307, 2014.

[41] D. Levin, S. Gannot, and E. A. P. Habets, "Direction-of-arrival estimation using acoustic vector sensors in the presence of noise," in *Proc. IEEE ICASSP*, pp. 105–108, 2011.

[42] M. Er and A. Cantoni, "Derivative constraints for broad-band element space antenna array processors," *IEEE Trans. Acoust., Speech, Signal Process.*, vol. 31, no. 6, pp. 1378–1393, 1983.

[43] H. F. Olson, "Gradient microphones," *J. Acoust. Soc. Am.*, vol. 17, no. 3, pp. 192–198, 1946.

[44] I. Cohen, J. Benesty, and J. Chen, "Differential Kronecker product beamforming," *IEEE/ACM Trans. Audio, Speech, Lang. Process.*, vol. 27, pp. 892–902, May. 2019.